applied sciences

MDPI

*Article*

# Broadband Metallic Carbon Nanotube Saturable Absorber for Ultrashort Pulse Generation in the 1500–2100 nm Spectral Range

**Maria Pawliszewska [1], Dorota Tomaszewska [1], Grzegorz Soboń [1], Anna Dużyńska [2], Mariusz Zdrojek [2] and Jarosław Sotor [1,*]**

[1] Laser & Fiber Electronics Group, Faculty of Electronics, Wrocław University of Science and Technology, Wybrzeże Wyspiańskiego 27, 50-370 Wrocław, Poland; maria.pawliszewska@pwr.edu.pl (M.P.); dorota.tomaszewska@pwr.edu.pl (D.T.); grzegorz.sobon@pwr.edu.pl (G.S.)

[2] Faculty of Physics, Warsaw University of Technology, Koszykowa 75, 00-662 Warsaw, Poland; anna.duzynska@pw.edu.pl (A.D.); mariusz.zdrojek@pw.edu.pl (M.Z.)

* Correspondence: jaroslaw.sotor@pwr.edu.pl

**Abstract:** Herein, we report on the possibility of ultrashort laser pulse generation in the broadband spectral range using a saturable absorber based on free-standing metallic carbon nanotube thin film. Erbium, thulium, and holmium-doped all-fiber lasers were mode-locked with a single saturable absorber containing a 300 nm thick material layer. Subpicosecond pulses were generated at 1559, 1938, and 2082 nm. Our work validates the broadband operation of metallic carbon nanotube-based saturable absorbers and highlights the suitable performance of nanomatematerial for ultrafast photonic applications.

**Keywords:** fiber laser; mode-locking; carbon nanotubes; saturable absorber; holmium-doped fiber; thulium-doped fiber; erbium-doped fiber



**Citation:** Pawliszewska, M.; Tomaszewska, D.; Soboń, G.; Dużyńska, A.; Zdrojek, M.; Sotor, J. Broadband Metallic Carbon Nanotube Saturable Absorber for Ultrashort Pulse Generation in the 1500–2100 nm Spectral Range. *Appl. Sci.* **2021**, *11*, 3121. https://doi.org/10.3390/app11073121

Academic Editor: Ju Han Lee

Received: 19 February 2021
Accepted: 23 March 2021
Published: 1 April 2021



## 1. Introduction

Carbon nanotubes, the one-dimensional form of graphite, maintain substantial popularity among the scientific community. Since their "re-invention" in 1991 [1], their unique electrical, mechanical, and optical properties have been extensively investigated and applied to a diverse range of devices, including transistors [2], photodetectors [3], optical switches [4], and gas sensors [5]. A report on the presence of saturable absorption in single-walled carbon nanotubes [6] led to the first demonstration of a nanomaterial-based ultrafast erbium-doped fiber laser in 2003 [7]. Since then, the family of nanomaterials exhibiting nonlinear optical absorption with ultrashort recovery times has expanded quickly. A pioneering two-dimensional material, graphene [8,9], was soon joined by graphene oxide [10], black phosphorus [11,12], transition metal monochalcogenides [13], transition metal dichalcogenides such as molybdenum disulfide [14,15] or tungsten disulfide [16,17], and topological insulators including bismuth telluride [18] and antimony telluride [19]. More recently, MXenes [20], bismuthene [21], and antimonene [22] were also found to show the desired nonlinear optical properties.

Despite the rapid growth in the field of nanomaterial-based saturable absorbers [23], carbon nanotubes maintain their established position due to their versatility, low cost, and ease of fabrication, as complex epitaxial processes are not required. Notably, free-standing films offer increased reliability and long-lasting performance in comparison to polymer-based composites [24]. A large number of diverse ultrafast laser setups based on carbon nanotube saturable absorbers present the material as a nearly universal mode locker. To date, they have been applied to fiber lasers operating in a broad range of wavelengths: From visible [25], through the entire near-infrared [26–28], to ~3 µm generated from ZBLAN fiber lasers [29,30]. Their broad transmission bandwidth allows to design lasers tunable over a 200 nm span [31], and the high damage threshold supports high

energy (up to 34 nJ) picosecond pulse generation at ∼1.5 µm [32]. The outstanding performance of the material enables the operation of more demanding ultrafast systems, such as stretched-pulse lasers [33,34] or resonators operating at gigahertz repetition rates [35]. Reports on mode-locking solid-state lasers that include sub-200 fs pulse generation at 1 µm [36] and 2 µm [37] present carbon nanotube-based saturable absorbers as a potential alternative to semiconductor saturable absorber mirrors (SESAMs).

The great majority of carbon nanotube-based ultrafast lasers demonstrated so far utilize either a naturally occurring mixture of metallic and semiconducting nanotubes, or purely semiconducting nanotubes. In the past, we have shown that a purely metallic single-walled carbon nanotube (m-SWCNT) thin film with interband transition $M_{11}$ at a maximum around 700 nm also exhibits effective saturable absorption in the ∼2 µm band [34]. In this work, we extend our previous findings by demonstrating that the saturable absorption outside the $M_{11}$ transition is broadband and supports ultrashort laser pulse generation in a >500 nm wide spectral range. For this purpose, a fully fiberized saturable absorber based on m-SWCNT thin film was fabricated. Erbium, thulium, and holmium-doped fiber lasers were mode-locked with a single saturable absorber with a 300 nm thick m-SWCNT layer, yielding sub-800 fs pulse generation in three wavelength regions: 1.5, 1.9, and 2.1 µm, respectively.

## 2. Saturable Absorber Fabrication and Characterization

### 2.1. Metallic-SWCNT Film Fabrication

Purely metallic carbon nanotube thin films were fabricated using the vacuum filtration method [38,39]. In the first step, a suspension of carbon nanotubes in a water and surfactant solution was prepared. Surfactant particles tend to adsorbate on the nanotube walls and prevent the aggregation of nanotubes in a liquid. Dry nanotubes from NanoIntegris (99% purity with tube diameters from 1.2 to 1.7 nm and lengths in the range of 0.1–4 µm) were added to a 1% water solution of sodium dodecyl sulfate to achieve a 0.004 mg/mL nanotube concentration. Later, such dispersion was sonicated using horn sonication, where it was placed in ice water for 1 h with 5 min breaks after each 10 min of sonication to prevent heating of the mixture. Next, the suspension was centrifuged at 12,000 rpm for 10 min to remove the unseparated nanotubes. An appropriate amount of as-prepared dispersion was filtered by the mixed cellulose membrane (MCE filter, 25 nm pore size, 25 mm diameter from Millipore) using a vacuum filtration setup that allowed to achieve a specified thickness of the m-SWCNT film, 150 and 300 nm. The thickness can be controlled by the volume of dispersion used for filtration, and was measured with a Bruker Icon atomic force microscope. Residual surfactant was washed away from the metallic carbon nanotube film by a large amount of deionized water and isopropyl alcohol. The m-SWCNT film on the membrane was gently dried and cut into 5 × 5 mm pieces, and then immersed in an acetone bath to dissolve the cellulose membrane. We note that the acetone was changed several times to complete the removal of the residual MCE. Then acetone was replaced by the 50% solution of isopropyl alcohol in water and each metallic carbon nanotube film was transferred to a fiber connector or a flat substrate (silicon covered by silicon dioxide or soda–lime glass) and dried under a nitrogen stream.

### 2.2. Metallic-SWCNT Film Characterization

To initially characterize the samples, the metallic carbon nanotube films were transferred onto flat substrates ($SiO_2$/Si for SEM and Raman measurements or soda–lime glass for optical absorption investigation). A scanning electron microscope (SEM) was used to analyze the topography and homogeneity of the film surface. Images for both film thicknesses are shown in Figure 1a,b, respectively (obtained with a Raith E-Line Plus microscope), demonstrating that the films have similar nanotube random composition independent of the film thickness. The nanotubes inside the films were tightly arranged, pure, without residual contamination. To confirm the type of nanotubes used, the optical absorption spectra of the samples were obtained (Figure 1c), measured in a 300–3000 nm

span using a Cary 5000 UV-Vis-NIR spectrometer. For both samples with different thicknesses, a typical interband transition $M_{11}$ for metallic single-walled carbon nanotubes with the maximum around 710 nm was observed. This result clearly confirms that the nanotubes exhibited a metallic type of conductivity. The Raman measurements were performed using an inVia Qontor Renishaw spectrometer with a 532 nm laser excitation line in a backscattering configuration. The results are shown in Figure 1d. The spectra present two main modes G and G′ (2D), typical for all carbon nanotubes, and a less intense RBM mode, which is characteristic for single-walled carbon nanotubes only. The relatively low intensity of the D mode indicates that the carbon nanotubes were clean without contamination and surfactant residues and contained slight defects, probably appearing as an effect of the nanotubes being closely packed inside the films.

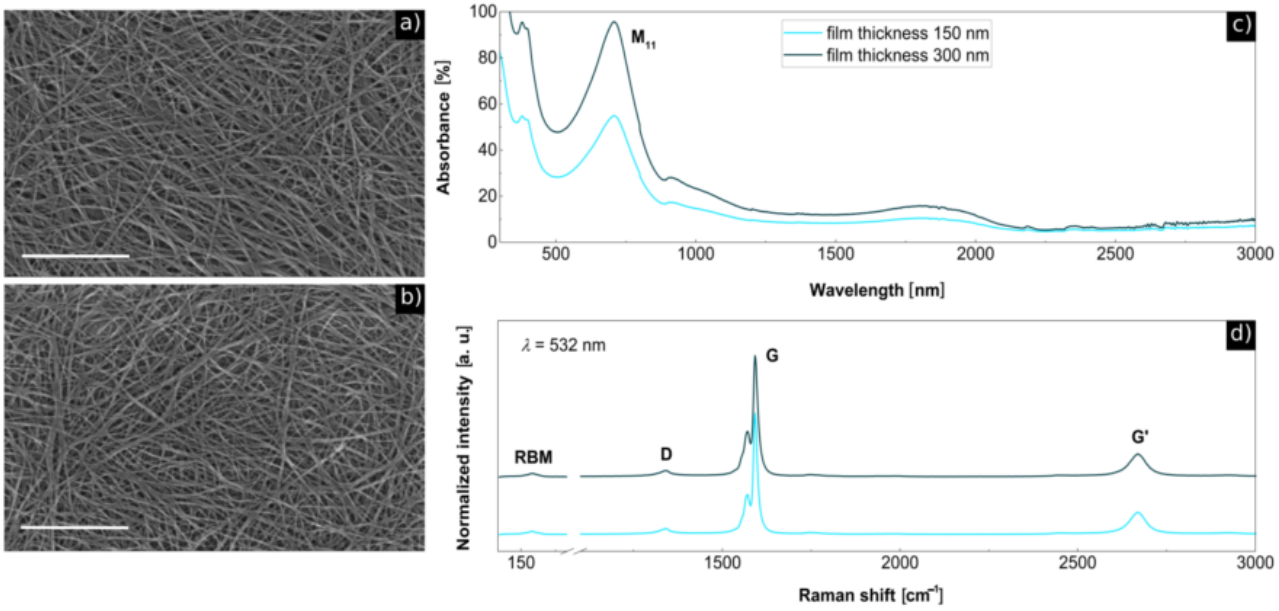


**Figure 1.** SEM image of the surface of m-SWCNT film with thicknesses of 150 nm (**a**) and 300 nm (**b**); scale bar represents 600 nm, Vis-IR absorbance spectra (**c**) and Raman spectra (**d**) of the films shown on SEM images. The m-SWCNT films were transferred on the $Si/SiO_2$ substrate and on soda–lime glass for the Raman and absorbance measurements, respectively.

### *2.3. Absorption in Metallic-SWCNT*

In general, the carbon nanotubes showed quite strong structured optical spectra owing to singularities in the electronic density of states and the transition between them, giving a strong enhancement of absorption peaks for certain energies. These absorption peaks were strongly related to the conductivity of the tubes due to the electronic band-to-band transition energies that were different for metallic and semiconducting films. Such an absorption peak for metallic tubes (shown in Figure 1c) is related to the first electronic transition $M_{11}$, which was the most intense. A second but much less intense absorption peak (however, not related to the electronic transition) was seen in the near IR range (∼1800 nm). The broadening of both peaks stemmed from tube–tube interaction and plasmon excitations [40].

### *2.4. Nonlinear Transmission of the m-SWCNT Saturable Absorber*

The free-standing m-SWCNT films were transferred to fiber connector tips, as shown in Figure 2a. To fabricate a fiberized saturable absorber, two fiber connectors with a 150 nm m-SWCNT thin film on each (a total of 300 nm thick material layer) were connected with a fiber adapter. Nonlinear optical transmission of the absorber was characterized in a fiber Z-scan style setup, incorporating an electronically controlled variable optical attenuator [41]. The measurement was conducted at 1560 nm (Figure 2b) and 1950 nm

(Figure 2c). The data were well fitted using a fast saturable absorber model [42] with the saturable absorption parameters indicated on corresponding graphs.

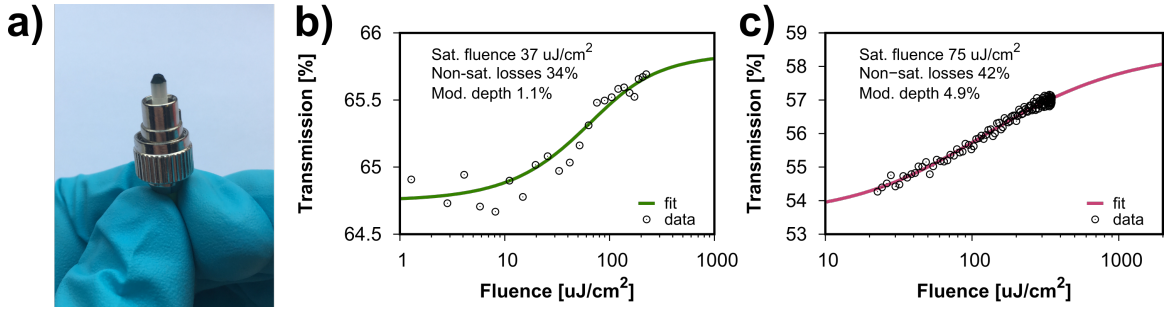


**Figure 2.** Metallic single-walled carbon nanotube (m-SWCNT) thin film deposited on a fiber connector tip (**a**). Nonlinear optical transmission of a 300 nm m-SWCNT saturable absorber fitted with a fast saturable absorber model measured at 1560 nm (**b**) and 1950 nm (**c**).

## 3. All-Fiber Lasers Mode-Locked with m-SWCNT Saturable Absorber

A single m-SWCNT saturable absorber containing 300 nm of the nanomaterial was integrated in three all-fiber lasers to experimentally verify its wideband nonlinear transmission. Erbium, thulium, and holmium-doped active fibers were used as a gain medium. The details of the investigated laser cavities are listed in Table 1. The lasers were operating in an all-anomalous (solitonic) dispersion regime. All three laser cavities employed a similar ring design incorporating a suitable wavelength division multiplexer, an isolator, and an output coupler (Figure 3). Polarization controllers were used to optimize the laser performance, as non-polarization maintaining fibers and components were used.

**Table 1.** Active fiber specification, output coupling ratio, and pump wavelength for the three investigated fiber lasers.

| **Dopant** | $Er^{3+}$ | $Tm^{3+}$ | $Ho^{3+}$ |
|---|---|---|---|
| **Fiber type** | OFS EDF80 | Nufern SM-TSF-5/125 | iXblue IXF-HDF-8-125 |
| **Fiber length** | 30 cm | 17 cm | 194 cm |
| **Output coupling ratio** | 10% | 10% | 30% |
| **Pump wavelength** | 980 nm | 1565 nm | 1940 nm |

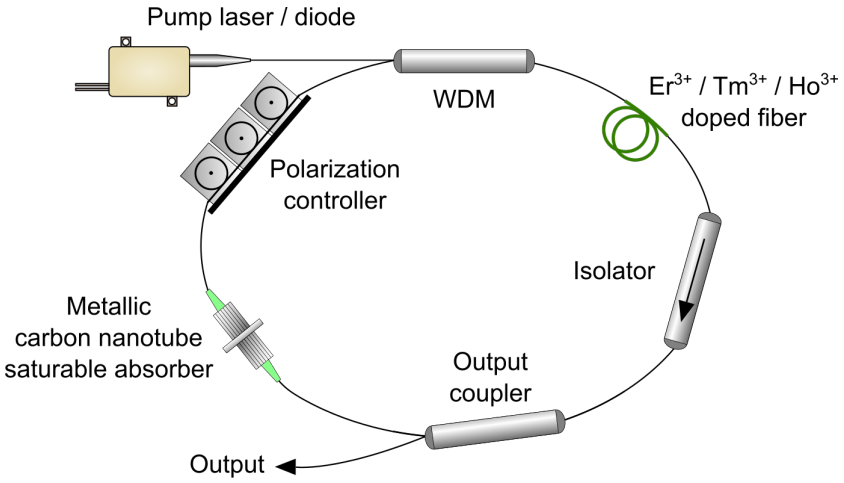


**Figure 3.** Schematic of the experimental laser setup. WDM, wavelength division multiplexer.

### *3.1. Erbium-Doped Fiber Laser*

The all-fiber erbium-doped laser cavity was directly pumped with a 980 nm semiconducting laser diode. Due to the relatively low modulation depth of the m-SWCNT at ~1560 nm, mode-locked operation was supported only in a narrow pump power range of 10–12 mW. A maximum average output power of 0.3 mW was observed. The generated optical spectrum centered at 1559 nm was 4.35 nm wide (Figure 4a). The autocorrelation trace presented in Figure 4b was fitted with a $\text{sech}^2$ curve, yielding a 617 fs pulse duration. The time bandwidth product of the emitted pulses was 0.33, indicating slight chirping of the solitons.

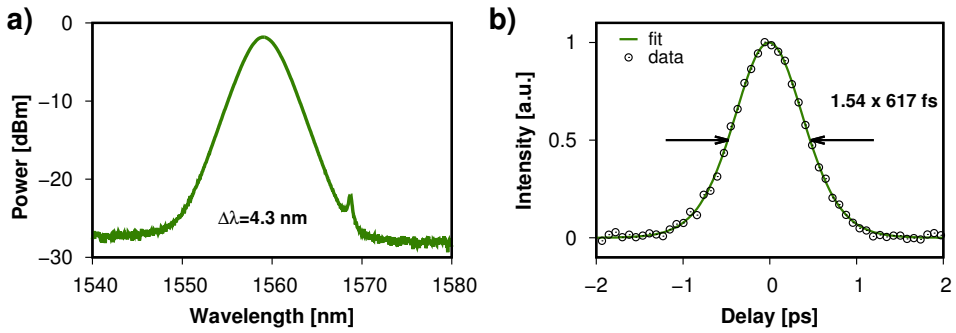


**Figure 4.** Optical spectrum (**a**) and autocorrelation trace with a $\text{sech}^2$ fitting (**b**) of the generated pulses.

### *3.2. Thulium-Doped Fiber Laser*

A thulium-doped fiber laser operating at 1938.7 nm was pumped by an erbium-doped fiber laser. At an average output power of 2.5 mW (pump power of 960 mW), a stable mode-locked operation was observed. The 6.1 nm wide optical spectrum exhibited some "dips" that were a result of strong water absorption lines present in the 1.9 µm region (Figure 5a). Pulse duration was of 713 fs, as shown in the autocorrelation trace presented in Figure 5b. The time bandwidth product of the pulses was equal to 0.36.

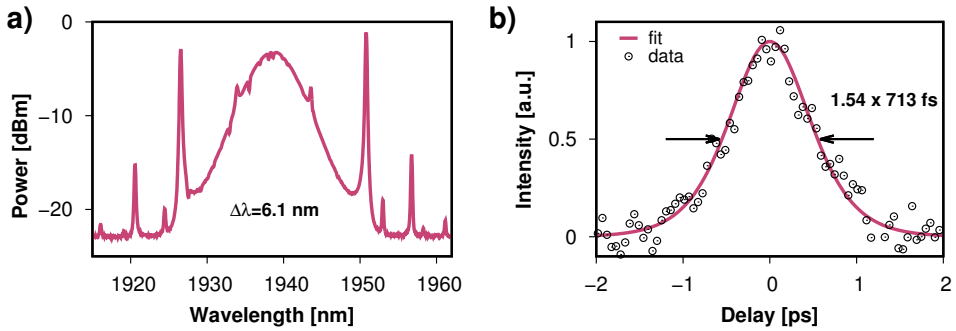


**Figure 5.** Optical spectrum (**a**) and autocorrelation trace with a $\text{sech}^2$ fitting (**b**) of the generated pulses.

### *3.3. Holmium-Doped Fiber Laser*

Lastly, a holmium-doped ring laser cavity was constructed. The resonator was pumped with an in-house-made linear thulium-doped fiber laser emitting a 1940 nm continuous wave radiation. The laser produced 717 fs pulses at a wavelength of 2082.4 nm (Figure 6a,b). The spectral width of the solitons was 6.35 nm, which corresponds to the time bandwidth product of 0.315, showing that the pulses were transform-limited. Up to 19.8 mW of the average output power was generated for a pump power of 1.1 W.

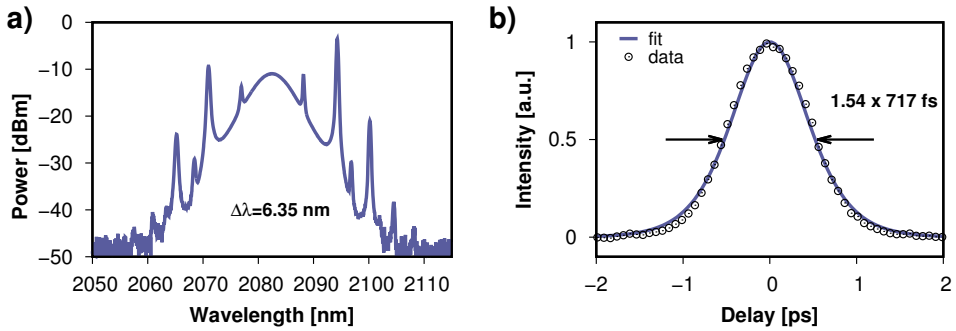


**Figure 6.** Optical spectrum (**a**) and autocorrelation trace with a sech$^2$ fitting (**b**) of the generated pulses.

The all-fiber cavities were designed to keep a comparable length of 3.8–4 m, which corresponds to repetition frequencies of 54.5, 52.2, and 54.3 MHz for the erbium, thulium, and holmium-doped fiber lasers, respectively. The radio frequency spectra of the fundamental repetition frequency, along with the spectra measured in a 1.25 GHz span (insets), are presented in Figure 7a–c. The high signal-to-noise ratios indicate the stable operation of the investigated mode-locked lasers. No pre- and postpulsing was observed in any of the cases.

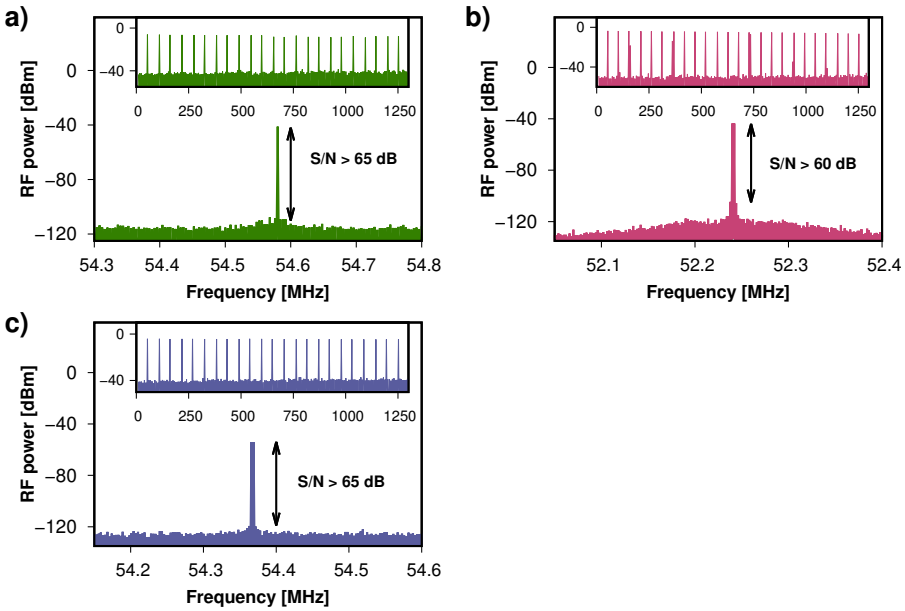


**Figure 7.** Radio frequency spectra measured around the fundamental mode and in a 1.25 GHz span (inset) of an erbium- (**a**), thulium- (**b**), and holmium-doped fiber laser (**c**).

Performance of the mode-locked lasers was characterized with the use of the following equipment: APE Pulsecheck autocorrelator (erbium laser), Femtochrome FR-103XL autocorrelator (thulium and holmium lasers), Yokogawa AQ6375 optical spectrum analyzer, Keysight EXA N9010A RF spectrum analyzer, and Discovery Semiconductors DSC2-50S 16 GHz photodiode.

## 4. Conclusions

In summary, we used a vacuum filtration method to fabricate a metallic single-walled carbon nanotube-based (m-SWCNT) saturable absorber. Nonlinear characterization of the 300 nm thin film yielded a modulation depth of 4.9%, while the linear transmission measurement presented the material as usable in a 1–3 µm wavelength span. We experimentally showed that a single m-SWCNT saturable absorber is capable of initiating mode-locking in fiber lasers operating at 1559, 1938, and 2082 nm. All three investigated lasers generated stable pulses with sub-800 fs durations. We highlighted that the same m-SWCNT saturable

absorber was used without failure in all three wavelength regions. Our results complement the current research on versatile and wideband saturable absorption in carbon nanotubes.

**Author Contributions:** Conceptualization, J.S.; thulium laser design, D.T. and G.S.; experimental investigation, M.P.; carbon nanotube film fabrication, A.D. and M.Z.; writing—original draft preparation, M.P. and A.D.; writing—review and editing, J.S. and G.S.; visualization, M.P. and A.D.; supervision, J.S. All authors read and agreed to the published version of the manuscript.

**Funding:** The Polish Ministry of Science and Higher Education (IP2015 073774) and The National Science Centre (2015/18/E/ST7/00296). One of the authors (Maria Pawliszewska) received financial support from the Polish National Science Centre in the form of a doctoral scholarship (2019/32/T/ST7/00223).

**Conflicts of Interest:** The authors declare no conflict of interest.

## References

1. Iijima, S. Helical microtubules of graphitic carbon. *Nature* **1991**, *354*, 56–58.
2. Noyce, S.G.; Doherty, J.L.; Cheng, Z.; Han, H.; Bowen, S.; Franklin, A.D. Electronic Stability of Carbon Nanotube Transistors Under Long-Term Bias Stress. *Nano Lett.* **2019**, *19*, 1460–1466.
3. Liu, Y.; Wang, F.; Wang, X.; Wang, X.; Flahaut, E.; Liu, X.; Li, Y.; Wang, X.; Xu, Y.; Shi, Y.; et al. Planar carbon nanotube–graphene hybrid films for high-performance broadband photodetectors. *Nat. Commun.* **2015**, *6*, 8589,
4. Tatsuura, S.; Furuki, M.; Sato, Y.; Iwasa, I.; Tian, M.; Mitsu, H. Semiconductor carbon nanotubes as ultrafast switching materials for optical telecommunications. *Adv. Mater.* **2003**, *15*, 534–537. [CrossRef]
5. Chopra, S.; McGuire, K.; Gothard, N.; Rao, A.; Pham, A. Selective gas detection using a carbon nanotube sensor. *Appl. Phys. Lett.* **2003**, *83*, 2280–2282. [CrossRef]
6. Chen, Y.C.; Raravikar, N.R.; Schadler, L.S.; Ajayan, P.M.; Zhao, Y.P.; Lu, T.M.; Wang, G.C.; Zhang, X.C. Ultrafast optical switching properties of single-wall carbon nanotube polymer composites at 1.55 µm. *Appl. Phys. Lett.* **2002**, *81*, 975–977.
7. Set, S.Y.; Yaguchi, H.; Tanaka, Y.; Jablonski, M.; Sakakibara, Y.; Rozhin, A.; Tokumoto, M.; Kataura, H.; Achiba, Y.; Kikuchi, K. Mode-locked fiber lasers based on a saturable absorber incorporating carbon nanotubes. In Proceedings of the OFC 2003 Optical Fiber Communications Conference, Atlanta, GA, USA, 23 March 2003; p. PD44.
8. Bao, Q.; Zhang, H.; Wang, Y.; Ni, Z.; Yan, Y.; Shen, Z.X.; Loh, K.P.; Tang, D.Y. Atomic-Layer Graphene as a Saturable Absorber for Ultrafast Pulsed Lasers. *Adv. Funct. Mater.* **2009**, *19*, 3077–3083. [CrossRef]
9. Sun, Z.; Hasan, T.; Torrisi, F.; Popa, D.; Privitera, G.; Wang, F.; Bonaccorso, F.; Basko, D.M.; Ferrari, A.C. Graphene Mode-Locked Ultrafast Laser. *ACS Nano* **2010**, *4*, 803–810. [CrossRef] [PubMed]
10. Lee, J.; Lee, J.H. A Passively Q-Switched Holmium-Doped Fiber Laser with Graphene Oxide at 2058 nm. *Appl. Sci.* **2021**, *11*, 407. [CrossRef]
11. Sotor, J.; Sobon, G.; Macherzynski, W.; Paletko, P.; Abramski, K.M. Black phosphorus a new saturable absorber material for ultrashort pulse generation. *Appl. Phys. Lett.* **2015**, *107*, 051108.
12. Luo, Z.C.; Liu, M.; Guo, Z.N.; Jiang, X.F.; Luo, A.P.; Zhao, C.J.; Yu, X.F.; Xu, W.C.; Zhang, H. Microfiber-based few-layer black phosphorus saturable absorber for ultra-fast fiber laser. *Opt. Express* **2015**, *23*, 20030–20039. [CrossRef]
13. Jhon, Y.I.; Lee, J.; Seo, M.; Lee, J.H.; Jhon, Y.M. Van der Waals Layered Tin Selenide as Highly Nonlinear Ultrafast Saturable Absorber. *Adv. Opt. Mater.* **2019**, *7*, 1801745. [CrossRef]
14. Zhang, H.; Lu, S.B.; Zheng, J.; Du, J.; Wen, S.C.; Tang, D.Y.; Loh, K.P. Molybdenum disulfide ($MoS_2$) as a broadband saturable absorber for ultra-fast photonics. *Opt. Express* **2014**, *22*, 7249. [CrossRef] [PubMed]
15. Woodward, R.; Kelleher, E.; Howe, R.; Hu, G.; Torrisi, F.; Hasan, T.; Popov, S.; Taylor, J. Tunable Q-switched fiber laser based on saturable edge-state absorption in few-layer molybdenum disulfide ($MoS_2$). *Opt. Express* **2014**, *22*, 31113–31122. [CrossRef] [PubMed]
16. Mao, D.; Wang, Y.; Ma, C.; Han, L.; Jiang, B.; Gan, X.; Hua, S.; Zhang, W.; Mei, T.; Zhao, J. WS2 mode-locked ultrafast fiber laser. *Sci. Rep.* **2015**, *5*, 7965. [CrossRef] [PubMed]
17. Wu, K.; Zhang, X.; Wang, J.; Li, X.; Chen, J. $WS_2$ as a saturable absorber for ultrafast photonic applications of mode-locked and Q-switched lasers. *Opt. Express* **2015**, *23*, 11453–11461. [CrossRef]
18. Zhao, C.; Zhang, H.; Qi, X.; Chen, Y.; Wang, Z.; Wen, S.; Tang, D. Ultra-short pulse generation by a topological insulator based saturable absorber. *Appl. Phys. Lett.* **2012**, *101*, 211106. [CrossRef]
19. Sotor, J.; Sobon, G.; Macherzynski, W.; Paletko, P.; Grodecki, K.; Abramski, K.M. Mode-locking in Er-doped fiber laser based on mechanically exfoliated $Sb_2Te_3$ saturable absorber. *Opt. Mater. Express* **2014**, *4*, 1. [CrossRef]
20. Dong, Y.; Chertopalov, S.; Maleski, K.; Anasori, B.; Hu, L.; Bhattacharya, S.; Rao, A.M.; Gogotsi, Y.; Mochalin, V.N.; Podila, R. Saturable Absorption in 2D $Ti_3C_2$ MXene Thin Films for Passive Photonic Diodes. *Adv. Mater.* **2018**, *30*, 1705714. [CrossRef]
21. Yang, Q.Q.; Liu, R.T.; Huang, C.; Huang, Y.F.; Gao, L.F.; Sun, B.; Huang, Z.P.; Zhang, L.; Hu, C.X.; Zhang, Z.Q.; et al. 2D bismuthene fabricated via acid-intercalated exfoliation showing strong nonlinear near-infrared responses for mode-locking lasers. *Nanoscale* **2018**, *10*, 21106–21115. [CrossRef]

22. Song, Y.; Liang, Z.; Jiang, X.; Chen, Y.; Li, Z.; Lu, L.; Ge, Y.; Wang, K.; Zheng, J.; Lu, S.; et al. Few-layer antimonene decorated microfiber: Ultra-short pulse generation and all-optical thresholding with enhanced long term stability. *2D Mater.* **2017**, *4*, 045010. [CrossRef]
23. Jiang, T.; Yin, K.; Wang, C.; You, J.; Ouyang, H.; Miao, R.; Zhang, C.; Wei, K.; Li, H.; Chen, H.; et al. Ultrafast fiber lasers mode-locked by two-dimensional materials: Review and prospect. *Photonics Res.* **2020**, *8*, 78–90. [CrossRef]
24. Kobtsev, S.; Ivanenko, A.; Gladush, Y.G.; Nyushkov, B.; Kokhanovskiy, A.; Anisimov, A.S.; Nasibulin, A.G. Ultrafast all-fibre laser mode-locked by polymer-free carbon nanotube film. *Opt. Express* **2016**, *24*, 28768–28773. [CrossRef]
25. Li, W.; Zhu, C.; Rong, X.; Wu, J.; Xu, H.; Wang, F.; Luo, Z.; Cai, Z. Bidirectional Red-Light Passively Q-Switched All-Fiber Ring Lasers With Carbon Nanotube Saturable Absorber. *J. Light. Technol.* **2018**, *36*, 2694–2701. [CrossRef]
26. Hasan, T.; Sun, Z.; Tan, P.; Popa, D.; Flahaut, E.; Kelleher, E.J.R.; Bonaccorso, F.; Wang, F.; Jiang, Z.; Torrisi, F.; et al. Double-Wall Carbon Nanotubes for Wide-Band, Ultrafast Pulse Generation. *ACS Nano* **2014**, *8*, 4836–4847. [CrossRef] [PubMed]
27. Kivistö, S.; Hakulinen, T.; Kaskela, A.; Aitchison, B.; Brown, D.P.; Nasibulin, A.G.; Kauppinen, E.I.; Härkönen, A.; Okhotnikov, O.G. Carbon nanotube films for ultrafast broadband technology. *Opt. Express* **2009**, *17*, 2358–2363. [CrossRef]
28. Chamorovskiy, A.; Marakulin, A.; Ranta, S.; Tavast, M.; Rautiainen, J.; Leinonen, T.; Kurkov, A.; Okhotnikov, O. Femtosecond mode-locked holmium fiber laser pumped by semiconductor disk laser. *Opt. Lett.* **2012**, *37*, 1448. [CrossRef] [PubMed]
29. Wei, C.; Lyu, Y.; Li, Q.; Kang, Z.; Zhang, H.; Qin, G.; Li, H.; Liu, Y. Wideband Tunable, Carbon Nanotube Mode-Locked Fiber Laser Emitting at Wavelengths Around 3 µm. *IEEE Photonics Technol. Lett.* **2019**, *31*, 869–872. [CrossRef]
30. Lü, Y.; Wei, C.; Zhang, H.; Kang, Z.; Qin, G.; Liu, Y. Wideband tunable passively Q-switched fiber laser at 2.8 µm using a broadband carbon nanotube saturable absorber. *Photonics Res.* **2019**, *7*, 14–18. [CrossRef]
31. Meng, Y.; Li, Y.; Xu, Y.; Wang, F. Carbon Nanotube Mode-Locked Thulium Fiber Laser With 200 nm Tuning Range. *Sci. Rep.* **2017**, *7*, 45109. [CrossRef]
32. Jeong, H.; Choi, S.Y.; Rotermund, F.; Cha, Y.H.; Jeong, D.Y.; Yeom, D.I. All-fiber mode-locked laser oscillator with pulse energy of 34 nJ using a single-walled carbon nanotube saturable absorber. *Opt. Express* **2014**, *22*, 22667–22672. [CrossRef]
33. Wang, J.; Cai, Z.; Xu, P.; Du, G.; Wang, F.; Ruan, S.; Sun, Z.; Hasan, T. Pulse dynamics in carbon nanotube mode-locked fiber lasers near zero cavity dispersion. *Opt. Express* **2015**, *23*, 9947–9958. [CrossRef]
34. Pawliszewska, M.; Dużyńska, A.; Zdrojek, M.; Sotor, J. Metallic carbon nanotube-based saturable absorbers for holmium-doped fiber lasers. *Opt. Express* **2019**, *27*, 11361–11369. [CrossRef] [PubMed]
35. Martinez, A.; Yamashita, S. Multi-gigahertz repetition rate passively modelocked fiber lasers using carbon nanotubes. *Opt. Express* **2011**, *19*, 6155–6163. [CrossRef] [PubMed]
36. Schmidt, A.; Rivier, S.; Steinmeyer, G.; Yim, J.H.; Cho, W.B.; Lee, S.; Rotermund, F.; Pujol, M.C.; Mateos, X.; Aguiló, M.; et al. Passive mode locking of Yb:KLuW using a single-walled carbon nanotube saturable absorber. *Opt. Lett.* **2008**, *33*, 729–731. [CrossRef]
37. Schmidt, A.; Koopmann, P.; Huber, G.; Fuhrberg, P.; Choi, S.Y.; Yeom, D.I.; Rotermund, F.; Petrov, V.; Griebner, U. 175 fs Tm:$Lu_2O_3$ laser at 2.07 µm mode-locked using single-walled carbon nanotubes. *Opt. Express* **2012**, *20*, 5313–5318. [CrossRef]
38. Wu, Z.; Chen, Z.; Du, X.; Logan, J.M.; Sippel, J.; Nikolou, M.; Kamaras, K.; Reynolds, J.R.; Tanner, D.B.; Hebard, A.F.; et al. Transparent, conductive carbon nanotube films. *Science* **2004**, *305*, 1273–1276. [CrossRef]
39. Duzynska, A.; Swiniarski, M.; Wroblewska, A.; Lapinska, A.; Zeranska, K.; Judek, J.; Zdrojek, M. Phonon properties in different types of single-walled carbon nanotube thin films probed by Raman spectroscopy. *Carbon* **2016**, *105*, 377–386. [CrossRef]
40. Reich, S.; Thomsen, C.; Maultzsch, J. *Carbon Nanotubes: Basic Concepts and Physical Properties*; John Wiley & Sons: Hoboken, NJ, USA, 2008.
41. Soboń, G. Mode-locking of fiber lasers using novel two-dimensional nanomaterials: Graphene and topological insulators [Invited]. *Photonics Res.* **2015**, *3*, A56. [CrossRef]
42. Kurtner, F.X.; Au, J.A.d.; Keller, U. Mode-locking with slow and fast saturable absorbers-what's the difference? *IEEE J. Sel. Top. Quantum Electron.* **1998**, *4*, 159–168. [CrossRef]